IET Communications

*Research Article*

IET Journals
The Institution of Engineering and Technology

# Asynchronous amplify-and-forward relay communications for underwater acoustic networks

ISSN 1751-8628
Received on 20th December 2014
Revised on 6th July 2015
Accepted on 30th August 2015
doi: 10.1049/iet-com.2014.1233
www.ietdl.org

*Rui Cao[1], Fengzhong Qu[2], Liuqing Yang[3] ✉*

[1]*Marvell Semiconductor Incorporation, Santa Clara CA 95054, USA*
[2]*Ocean College, Zhejiang University, Zhoushan 316021, People's Republic of China*
[3]*Department of Electrical and Computer Engineering, Colorado State University, Fort Collins CO 80523, USA*
✉ *E-mail: lqyang@engr.colostate.edu*

**Abstract:** Underwater acoustic communications (UAC) feature frequency-dependent signal attenuation, long propagation delay and doubly-selective fading. Thus the design of reliable UAC protocols is challenging. On the other hand, cooperative relay communications, which have been extensively studied in terrestrial environments, are promising paradigms for reliable communications. However, their application to UAC has not been thoroughly explored. In this study, the authors will design an asynchronous relaying protocol to achieve reliable underwater communications. This new scheme accounts for and takes advantage of the unique characteristics of UAC channels. To avoid time synchronisation difficulty in UAC, and facilitate energy-efficient relay processing, asynchronous amplify-and-forward relaying is adopted in the protocol. In addition, precoded orthogonal frequency division multiplexing is chosen to address the frequency selectivity issue in UAC, while collecting ample multipath diversity provided by the channel and enabled by the asynchronous relaying design. To demonstrate the performance of the protocol, the end-to-end signal-to-noise ratio is derived, the average pair-wise error probability is evaluated and the maximum collectable diversity is also proven. Simulations and comparisons are presented to corroborate the analyses and design.

## 1 Introduction

Advances in underwater networking technologies are the foundation of various oceanic applications, such as environment monitoring, off-shore exploration and tactical surveillance [1, 2]. Underwater acoustic communications (UAC), which adopt acoustic waves as the information carrier, become a promising communication technique. However, the unique features of acoustic signal propagation and the underwater environment pose new research challenges to wireless communications. On one hand, long and variant delay, caused by slow acoustic signal propagation (around 1500 m/s) and environmental effects, hampers accurate time synchronisation and well-coordinated medium access [2–6]. On the other hand, the doubly-selective nature of UAC channel induces error-prone transmissions [7]. Therefore, the design of UAC protocols needs to achieve efficient bandwidth utilisation and reliable data transmission with relaxed synchronisation requirement.

In terrestrial wireless communications, cooperative relay communications have been extensively studied to provide reliable data transmission with extended distances [8, 9]. To enhance the communication between the source and the destination, several relays are employed in between to assist the communication. Space diversity can be achieved through smart relay processing and collaboration, and the data reception at the destination can be significantly improved with proper design of the detection scheme. Relay communication furnishes a promising solution for long-range reliable UAC. Due to the limited bandwidth and power, various studies have been conducted to optimise the underwater relay communication schemes [10–15]. The optimal relay placement are studied based on different optimisation criteria, such as transmission delay [11], power consumption [12], signal-to-noise ratio (SNR) [11, 13], error performance [13] and etc. In [10, 16], the optimal power policy is investigated to maximise end-to-end system data rate for different system setup. In [17], a novel multi-hop communication architecture based on progressive encoding is proposed for underwater big data delivery. Abstract physical layer transmission is considered in this scheme. In [15], a single-relay selection scheme is designed to enhance underwater communication performance. Besides resource optimisation, due to peculiar UAC characteristics, the relay-aided (RA-) UAC protocol design needs to relax relay synchronisation requirement while retaining the spectrum efficiency.

In the literature, asynchronous relay communications has been exploited to achieve better end-to-end capacity. In this type of scheme, all relays forward the source data to the destination in the same time frame. Compared with orthogonal relay channel allocation [6, 8, 9], the spectrum efficiency is much improved. However, the uncoordinated relay transmission results in more inter-symbol-interference (ISI), which poses challenges to the reliable reception at the destination. In terrestrial environments, the relays are accurately synchronised, simultaneous transmission loses space diversity. Several protocols have been proposed to collect delay diversity by introducing artificial random delay at each relay. In [18], an asynchronous relaying scheme is designed by introducing artificial delay at the relays. For a single carrier communication system with Rayleigh fading channel, the diversity achieved with a minimum mean square error detector is analysed based on the outage probability. In [6], a relay transmission scheme is designed for a two-relay system that can tolerate large propagation delay. In [19, 20], multi-carrier asynchronous relay communication protocols are design for Rayleigh fading channels with ISI. Plain orthogonal frequency division multiplexing (OFDM) is adopted in [20], and maximum ratio combining is implemented to achieve diversity. OFDM with convolution codes is utilised in [19].

In underwater relay communications, due to slow acoustic signal propagation and random delay variance, accurate relay synchronisation is extremely difficult. Asynchronous relay transmission naturally fits in the underwater relay communications. However, the existing schemes do not fully achieve the delay diversity ([20]) or induces data rate penalty ([19]), which is critical for limited underwater capacity. Several RA-UAC protocols have

been proposed in the literature to address the time synchronisation difficulty. In [4], an Alamouti-type cooperative scheme with 2 or 4 relays is designed based on time-reversal distributed space-time block code. By incorporating effects of relaying asynchronism into equivalent delayed multipath channels, the scheme is resistant to timing errors among relays. However, it is still sensitive to propagation delay variance within each Alamouti pair, and the asynchronous direct-link transmission is not considered. In addition, the Alamouti-type design retains space diversity, but no multipath diversity is collected. In [21, 22], asynchronous protocols with a single relay are analysed. In these schemes, the relay forwards source signals to the destination right after processing. At the destination, the asynchronism between the direct link and the relay link is resolved under an ideal assumption that signals received from the source and the relay can be perfectly separable.

In this paper, we propose a practical asynchronous relaying protocol tailored for UAC: asynchronous amplify-and-forward (AF) relaying with precoded OFDM (AsAP). The AsAP scheme combats time asynchronism with practical assumptions, and achieves reliable data communications by utilising the sparse nature of UAC channels [23]. Consider a dual-hop multi-relay UAC system, where the source signals are modulated with grouped linear constellation precoding (GLCP) OFDM [24]. All relays simply amplify the received signal and forward to the destination in an asynchronous mode. Full-duplex transmission can be implemented at the relays. With these designs, the AsAP protocol can address the UAC difficulties while taking advantage of the unique UAC features. On one hand, the asynchronous AF relaying avoids time synchronisation difficulty and facilitates simple relay processing. On the other hand, the precoded OFDM resolves frequency selectivity issue of the UAC channel and collects both space and multipath diversity. Due to the sparsity of underwater channels [23], the asynchronism naturally converts space diversity into resolvable multipath diversity, which can be collected by precoded OFDM. In addition, the GLCP retains the high spectrum efficiency without data rate loss. To further improve the efficiency, full-duplex relay transmission [25, 26] can be adopted in AsAP, thanks to the separation of hydrophones and transducers in UAC devices and the directional transmission of transducers [21]. The analysis of full-duplex AsAP will not be included in this paper. To demonstrate the merits of our AsAP protocol, we derive the end-to-end SNR, the average pair-wise error probability (PEP) and the maximum collectable diversity (MCD) gain. Our protocol achieved reliable communication with high diversity without suffering data rate loss. In addition, simulations and comparisons are provided to verify the performance of our AsAP protocol, and to reveal the effects of system parameters, such as number of relays and channel taps, and amplification factors.

The contribution of this paper lies in the following aspects. First, we derived the performance for relay communications with GLCP. The result is only available for point-to-point communications in [24]. Second, we analysed the achievable diversity of GLCP relay systems with non-uniform channel variances. In the literature, the diversity study assumes equal tap variance. However, underwater multipath channel is featured with decaying energy profile, where each channel delay tap has a unique propagation-distance-dependent variance. Third, multiple AF amplifying protocols are designed and the effect of different relay amplifying protocol is studied.

The rest of the paper is organised as follows. We first introduce the underwater acoustic system and channel in Section 2. The AsAP protocol is presented in Section 3. The performance analysis and simulation results are illustrated in Sections 4 and 5, respectively. Finally, summarising remarks will be given in Section 6.

*Notation:* In this paper, bold upper-case and lower-case letters are used for matrices and vectors, respectively; $(\cdot)^{\mathrm{H}}$ denotes the Hermitian operation; diag($\boldsymbol{v}$) is a diagonal matrix with $\boldsymbol{v}$ as its diagonal entries; $|\cdot|$, $\|\cdot\|$ and det($\cdot$) represents the absolute value, Euclidean distance and determinant, respectively; 'mod' is used as the modulo operator; $\mathbb{E}_b[a]$ is referred to as the average of variable $a$ conditioned on variable $b$; $\mathcal{CN}(\mu, \sigma^2)$ stands for a complex Gaussian distribution with mean $\mu$ and variance $\sigma^2$.

## 2 Underwater channel model

Compared with terrestrial radio frequency (RF) channels, UAC channels exhibit different features: frequency-dependent signal attenuation and sparse multipath.

### 2.1 Signal attenuation model

In the literature, empirical underwater acoustic signal propagation models are established [27], and later introduced into UAC [28]. Underwater acoustic signal attenuation $\mathcal{A}$ is both distance $D$ and frequency $f$ dependent

$$\mathcal{A}(D, f) = D^k \cdot a(f)^{\mathrm{D}}, \tag{1}$$

where $k$ is the path loss exponent which reflects the geometry of acoustic signal propagation. For example, $k=2$ is used for spherical spreading, $k=1$ is for cylindrical spreading, and $k=1.5$ is referred to as practical spreading. In this paper, $k=1.5$ is used if not otherwise specified. The frequency dependency is captured by $a(f)$, which is given by Thorp's formula [27]

$$10\log a(f) = \frac{0.11 f^2}{1+f^2} + \frac{44 f^2}{4100+f^2} + 2.75\times 10^{-4} f^2 + 0.003. \tag{2}$$

In (1) and (2), the units are: $D$ in km, $f$ in kHz.

### 2.2 Multipath channel model

Due to the slow acoustic signal propagation and discrete reflections from the surface/bottom, UAC channels also feature long yet spare channel delay taps. Due to the slow propagation of acoustic waves underwater ($v_{\mathrm{acoustic}} \doteq 1500$ m/s), signals reflected from the sea surface and/or bottom arrive at the receiver with distinct delays. This results in a sparse multipath channel [29]. Each reflection path obeys the propagation rule in (1). Thus a UAC channel of length $L$ is represented as $\boldsymbol{h} := [h_0, \ldots, h_{L-1}]$, within which only $L_{\mathrm{nz}}$ taps are non-zero. Each non-zero tap $h_l$, $l \in \{l_0, \ldots, l_{L_{\mathrm{nz}}-1}\}$ corresponds to one arrival, and is independently complex Gaussian distributed with zero mean and variance $\sigma_l^2$, that is, $h_l \sim \mathcal{CN}(0, \sigma_l^2)$ [4]. The variance is computed as

$$\sigma_l = \frac{\Gamma_l}{\sqrt{\mathcal{A}(d_l, f)}}, \tag{3}$$

where $\mathcal{A}(d_l, f)$ is the attenuation computed as in (1) and $d_l$ is the propagation distance of the $l$th arrival, which is determined by the number of reflections with the channel geometry described in [30]. $\Gamma_l$ is the reflection loss of acoustic waves. In addition, each non-zero tap is characterised by its delay time $\tau_l = d_l / v_{\mathrm{acoustic}}$. In Fig. 1, we plot a snapshot of the sparse acoustic channel in sea trial RACE08 at a 1000 m transmission distance [7].

The unique features of underwater acoustic channels have great impacts on the protocol design of RA-UAC. We will design a practical RA-UAC protocol in the next section.

## 3 AsAP relay protocol design

In RA-UAC, accurate time synchronisation among all nodes is hindered by the slow and variant signal propagation, and the characteristic of the UAC channel is sparse and multipath. Thus asynchronous relaying scheme is proposed in our protocol. In terrestrial RF communications with dense multipath, this asynchronism will easily cause diversity loss due to multipath collision. In our protocol design, however, we deliberately choose to allow such asynchronism to take advantage of the sparse nature of underwater acoustic channels. In fact, by this simple asynchronous approach, space diversity is transformed into


*IET Commun.*, 2016, Vol. 10, Iss. 6, pp. 677–684

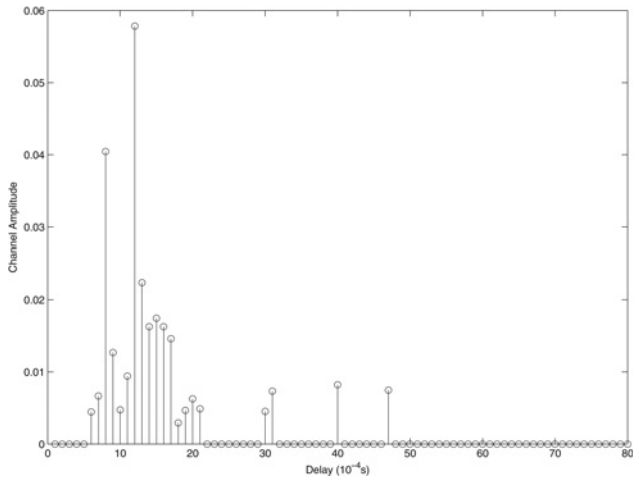


**Fig. 1** *Example of underwater acoustic channel estimated from RACE08 sea trial at a transmission distance of D = 1000 m*

multipath diversity. To collect the rich multipath diversity in RA-UAC, we resort to the GLCP OFDM technique. Hence, there is no need for any special means of dealing with space diversity. The resultant scheme is termed as asynchronous amplify-and-forward relaying with precoded OFDM (AsAP).

### 3.1 System setup

In AsAP, we consider a dual-hop multi-relay system with one source node $s$, $R$ relay nodes $r \in \{1,\ldots,R\}$ and one destination node $d$, shown in Fig. 2. The AsAP end-to-end transmission consists of three phases. First, the source generates information symbols modulated with GLCP OFDM, and broadcasts them. In the second phase, each relay amplifies its received signal and asynchronously forwards it to the destination right after processing. Finally, the destination collects all asynchronously arriving signals and decodes them. The signal processing flowchart for one equivalent source-relay-destination (S-R-D) path is shown in Fig. 2. The detailed processing at each phase will be elaborated in the following section.

In AsAP systems, we assume that the channel for each link is block-stationary, and the additive noise is white complex Gaussian with zero mean and variance $\mathcal{N}_0$ as in [4]. In addition, to facilitate our system description, we adopt the following notations. $\boldsymbol{F}$ denotes the $N$-point fast Fourier transformation (FFT) matrix with $\boldsymbol{F}(p, q) = (1/\sqrt{N})\exp(-j2\pi pq/N)$, $p, q \in \{0, \ldots, N-1\}$, and $\boldsymbol{F}^{\mathrm{H}}$ is the inverse FFT (IFFT) matrix. In addition, $\boldsymbol{h}_{i,j}$, $i, j \in \{s, r, d\}$ represents the channel vector between node $i$ and $j$, and $\tilde{\boldsymbol{h}}_{i,j} = \boldsymbol{F}\boldsymbol{h}_{i,j}$ is the frequency domain (FD) channel response.

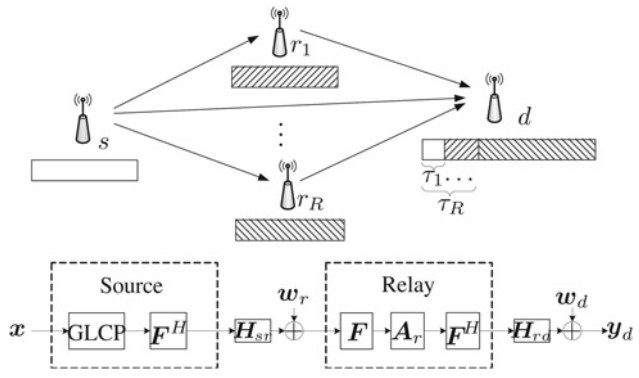


**Fig. 2** *System topology for the AsAP protocol with frequency-domain amplification*

### 3.2 Transmission protocol

*3.2.1 Source transmission:* At the source, each OFDM symbol $\tilde{\boldsymbol{x}}$ is precoded with GLCP and then broadcast to the relays and the destination. The GLCP consists of two steps: grouping and precoding. We adopt the optimal grouping rule in [24], which maximises diversity and coding gain. The grouping is performed as follows. For a precoding size $K$, the data symbol $\tilde{\boldsymbol{x}}$ of length $N$ is first divided into consecutive $K$ blocks, each of size $M$, then the $m$th ($m \in \{1,\ldots,M\}$) element from each block is selected to form a group, denoted by a vector $\tilde{\boldsymbol{x}}_{\mathrm{m}}$. All possible group vectors form a finite constellation set $\mathcal{A}_K$. This procedure can be mathematically represented as: $\tilde{\boldsymbol{x}}_{\mathrm{m}} = \boldsymbol{\Psi}_{\mathrm{m}}\tilde{\boldsymbol{x}}$, where $\boldsymbol{\Psi}_{\mathrm{m}} := \boldsymbol{I}_N(\mathcal{I}_{\mathrm{m}}, :)$ is a $K \times N$ selection matrix with the $K$ rows chosen from an $N \times N$ identity matrix $\boldsymbol{I}_N$, and the index of the $K$ rows are defined in the set $\mathcal{I}_{\mathrm{m}}$. For optimal grouping, each row set is chosen as $\mathcal{I}_{\mathrm{m}} := \{m, m+K, \ldots, m+(K-1)M\}$. In the second step, each group vector $\tilde{\boldsymbol{x}}_{\mathrm{m}}$ is encoded with precoder matrix $\boldsymbol{\Theta}_K$ of size $K \times K$. To achieve the maximum diversity gain, $\boldsymbol{\Theta}_K$ is designed as in [24]. Then, the coded groups are reassembled to form the precoded symbol $\tilde{\boldsymbol{x}}_{\mathrm{s}}$. The entire GLCP process can be represented as

$$\tilde{\boldsymbol{x}}_{\mathrm{s}} = \sum_{m=1}^{M} \boldsymbol{\Psi}_{\mathrm{m}}^{\mathrm{T}}\boldsymbol{\Theta}\boldsymbol{\Psi}_{\mathrm{m}}\tilde{\boldsymbol{x}}. \tag{4}$$

To overcome ISI, cyclic prefix (CP) is inserted after IFFT. Then the generated time-domain symbol $\boldsymbol{x}_{\mathrm{s}}$ is broadcast to the relays and destination with transmit power $\mathcal{P}_{\mathrm{s}}$. The CP length is properly chosen to address possible asynchronous delay $\tau$, which is specified in the following part. To achieve better spectrum efficiency, coarse time synchronisation can be implemented for smaller $\tau$.

*3.2.2 Relay forwarding:* After propagating through the source-to-relay (S-R) channel, the received signal $\boldsymbol{y}_{\mathrm{r}}$ at relay $r$ can be represented as

$$\boldsymbol{y}_{\mathrm{r}} = \boldsymbol{H}_{\mathrm{sr}}\sqrt{\mathcal{P}_{\mathrm{s}}}\boldsymbol{x}_{\mathrm{s}} + \boldsymbol{n}_{\mathrm{r}}, \tag{5}$$

where $\boldsymbol{H}_{\mathrm{sr}}$ is the toeplitz matrix of the S-R channel vector $\boldsymbol{h}_{\mathrm{sr}}$ and $\boldsymbol{n}_{\mathrm{r}}$ is the noise at relay $r$.

To compensate the S-R channel fading, each relay amplifies the received signal before forwarding it to the destination. The amplification factor $\boldsymbol{A}_{\mathrm{r}}$ is a diagonal matrix with the amplification magnitude for each subcarrier/bit as its diagonal entry, whose value is chosen to assure that the average/instantaneous relaying signal power complies with relay transmit power limit $\mathcal{P}_{\mathrm{r}}$. Depending on different performance and computation requirements, the amplification can be implemented either in time domain (TD) or in FD.

In TD amplification, the relay forwarding signal $\boldsymbol{x}_{\mathrm{r}}$ is generated by multiplying the amplification matrix directly to the time-domain received signal, that is, $\boldsymbol{x}_{\mathrm{r}} = \boldsymbol{A}_{\mathrm{r}}\boldsymbol{y}_{\mathrm{r}}$. The amplification factor $\boldsymbol{A}_{\mathrm{r}}$ is determined to satisfy the power constraint of the entire transmit symbol. Thus the amplification magnitude $A_{\mathrm{r}}$ is the same for each bit in TD, namely $\boldsymbol{A}_{\mathrm{r}} = A_{\mathrm{r}}\boldsymbol{I}$, where $\boldsymbol{I}$ is an identity matrix. We consider two TD amplification schemes: the fixed amplification (TD-FA) and the instantaneous amplification (TD-IA). In TD-FA, the amplification factor is computed by complying with the average power constraint: $\mathbb{E}\left(|A_{\mathrm{r}}|^2||\boldsymbol{y}_{\mathrm{r}}||^2\right) = (L_{\mathrm{CP}} + N)\mathcal{P}_{\mathrm{r}}$. Thus the amplification magnitude can be pre-computed with the average channel power $\mathbb{E}(||\boldsymbol{h}_{\mathrm{sr}}||^2)$ and noise variance $\mathcal{N}_0$:

$$A_{\mathrm{r,TD-FA}} = \sqrt{\frac{\mathcal{P}_{\mathrm{r}}}{\mathcal{P}_{\mathrm{s}}\mathbb{E}(||\boldsymbol{h}_{\mathrm{sr}}||^2) + \mathcal{N}_0}}. \tag{6}$$

For TD-IA, the amplification factor will satisfy the instantaneous power constraint for each OFDM symbol, that is, $|A_{\mathrm{r}}|^2||\boldsymbol{y}_{\mathrm{r}}||^2 = (L_{\mathrm{CP}} + N)\mathcal{P}_{\mathrm{r}}$. Thus the amplification magnitude is

computed as,

$$A_{\mathrm{r,TD-IA}} = \frac{\sqrt{(L_{\mathrm{CP}} + N)\mathcal{P}_{\mathrm{r}}}}{\|\boldsymbol{y}_{\mathrm{r}}\|}. \tag{7}$$

With TD amplification, the maximum tolerable asynchronous delay (MTAD) $\tau_{\mathrm{m}}$ at the destination will be the difference between the CP length and the greatest S-R-D channel length: $\tau_{\mathrm{m}} = L_{\mathrm{CP}} - \max_{\mathrm{r}\in\{1,\ldots,R\}} \{L_{\mathrm{s,r}} + L_{\mathrm{r},d} - 1\}$. To increase the tolerance to timing asynchronism, each relay can update the forwarding signal's CP with the last $L_{\mathrm{CP}}$ samples of the amplified signal. Then the MTAD is prolonged to

$$\tau_{\mathrm{m}} = L_{\mathrm{CP}} - \max_{r\in\{1,\ldots,R\}} L_{\mathrm{r},d}. \tag{8}$$

In FD amplification, the received signal is first transformed to the FD representation, and then each subcarrier is amplified according to its signal attenuation. Through normal CP removal and FFT, the frequency-domain signal $\tilde{\boldsymbol{y}}_{\mathrm{r}}$ is represented as

$$\tilde{\boldsymbol{y}}_{\mathrm{r}} = \boldsymbol{D}_{\mathrm{sr}}\sqrt{\mathcal{P}_{\mathrm{s}}}\tilde{\boldsymbol{x}}_{\mathrm{s}} + \tilde{\boldsymbol{n}}_{\mathrm{r}}, \tag{9}$$

where $\boldsymbol{D}_{\mathrm{sr}} = \mathrm{diag}(\tilde{\boldsymbol{h}}_{\mathrm{sr}}) = \mathrm{diag}(\boldsymbol{F}\boldsymbol{h}_{\mathrm{sr}})$ is the diagonal S-R channel matrix, and $\tilde{\boldsymbol{n}}_{\mathrm{r}} = \boldsymbol{F}\boldsymbol{n}_{\mathrm{r}}$ is the FD noise vector. The FD amplified signal is computed as: $\tilde{\boldsymbol{x}}_{\mathrm{r}} = \boldsymbol{A}_{\mathrm{r}}\tilde{\boldsymbol{y}}_{\mathrm{r}}$, and the TD forwarding signal is generated by performing IFFT of $\tilde{\boldsymbol{x}}_{\mathrm{r}}$ and CP insertion. In FD amplification, the MTAD at the destination is the same as the TD amplification scheme with CP update in (8).

We also consider two FD amplification schemes: the subcarrier amplification (FD-SA) and the group amplification (FD-GA). In FD-SA scheme, the power constraint is imposed on each subcarrier $i$, that is, $|\boldsymbol{A}_{\mathrm{r}}(i,i)\tilde{\boldsymbol{y}}_{\mathrm{r}}(i)|^2 = \mathcal{P}_{\mathrm{r}}$. Thus the amplification factor is obtained as

$$\boldsymbol{A}_{\mathrm{r,FD-SA}} = \mathrm{diag}\left(\frac{\sqrt{\mathcal{P}_{\mathrm{r}}}}{|\tilde{\boldsymbol{y}}_{\mathrm{r}}|}\right). \tag{10}$$

In FD-GA, because of the GLCP scheme adopted in our protocol, it is also reasonable to constrain the transmit power of each precoding group to $K\mathcal{P}_{\mathrm{r}}$, that is, $A_{\mathrm{m}}||\boldsymbol{\Psi}_{\mathrm{m}}\tilde{\boldsymbol{y}}_{\mathrm{r}}||^2 = K\mathcal{P}_{\mathrm{r}}$, where $A_{\mathrm{m}}$ is the amplification magnitude for group $m$. Then we can obtain the amplification factor as

$$\boldsymbol{A}_{\mathrm{r,FD-GA}} = \sum_{m=1}^{M} \boldsymbol{\Psi}_{\mathrm{m}}^{\mathrm{T}} \frac{\sqrt{K\mathcal{P}_{\mathrm{r}}}}{||\boldsymbol{\Psi}_{\mathrm{m}}\tilde{\boldsymbol{y}}_{\mathrm{r}}||}\boldsymbol{e}_K, \tag{11}$$

where $\boldsymbol{e}_K = [1, \ldots, 1]^{\mathrm{T}}$ is an all-one column vector of size $K$.

In these four amplification schemes, the TD-FA scheme possess the feature of simple implementation with less signal processing; the other three schemes are based on instantaneous signal information, thus more signal processing is needed. This will induce extra energy consumption and processing delay, but better performance can be achieved.

Finally, after amplification, all relays will forward the signals to the destination in the same time slot in an asynchronous mode.

*3.2.3 Destination decoding:* At the destination, the relayed signals arrive with random delays, which originate from relay location difference, signal propagation variance and random signal processing delay at each relay. Denote the delay of signal from relay $r$ with respect to the arrival time of the direct-link signal as $\tau_{\mathrm{r}}$. Assume that the maximum delay among all relays is less than MTAD $\tau_{\mathrm{m}}$. Then after normal OFDM processing, we can express the FD received symbol $\tilde{\boldsymbol{y}}_d$ as

$$\tilde{\boldsymbol{y}}_d = \boldsymbol{D}_{\mathrm{eq}}\sqrt{\mathcal{P}_{\mathrm{s}}}\tilde{\boldsymbol{x}}_{\mathrm{s}} + \tilde{\boldsymbol{n}}_{\mathrm{eq}}, \tag{12}$$

where $\boldsymbol{D}_{\mathrm{eq}}$ is the equivalent end-to-end diagonal channel matrix, which is computed as

$$\boldsymbol{D}_{\mathrm{eq}} = \boldsymbol{D}_{sd} + \sum_{r=1}^{R} \boldsymbol{\Omega}_{\mathrm{r}}\boldsymbol{D}_{\mathrm{r}d}\boldsymbol{A}_{\mathrm{r}}\boldsymbol{D}_{\mathrm{sr}}. \tag{13}$$

In this equation, $\boldsymbol{D}_{sd} = \mathrm{diag}(\tilde{\boldsymbol{h}}_{sd}) = \mathrm{diag}(\boldsymbol{F}\boldsymbol{h}_{sd})$ and $\boldsymbol{D}_{\mathrm{r}d} = \mathrm{diag}(\tilde{\boldsymbol{h}}_{\mathrm{r}d}) = \mathrm{diag}(\boldsymbol{F}\boldsymbol{h}_{\mathrm{r}d})$ are the diagonal S-D and R-D channel matrices, respectively. Besides, $\boldsymbol{\Omega}_{\mathrm{r}}$ is an $N\times N$ diagonal delay matrix for relay $r$, which multiplies each subcarrier $i$ with a corresponding phase factor $\boldsymbol{\Omega}_{\mathrm{r}}(i,i) = \exp(-j2\pi i\tau_{\mathrm{r}}/N)$. In addition, $\tilde{\boldsymbol{n}}_{\mathrm{eq}}$ is the equivalent FD noise vector computed as

$$\tilde{\boldsymbol{n}}_{\mathrm{eq}} = \tilde{\boldsymbol{n}}_{\mathrm{d}} + \sum_{r=1}^{R} \boldsymbol{\Omega}_{\mathrm{r}}\boldsymbol{D}_{\mathrm{r}d}\boldsymbol{A}_{\mathrm{r}}\tilde{\boldsymbol{n}}_{\mathrm{r}}, \tag{14}$$

where $\tilde{\boldsymbol{n}}_d = \boldsymbol{F}\boldsymbol{n}_d$ is the FD noise at the destination$_R$ Note that the equivalent noise $\tilde{\boldsymbol{n}}_{\mathrm{eq}}$ has a covariance of $\boldsymbol{\Delta}_n = \boldsymbol{I} + \sum_{r=1} |\boldsymbol{D}_{\mathrm{r}d}\boldsymbol{A}_{\mathrm{r}}|^2$.

Assume perfect channel state information is known at the destination, the decision statistic is computed by whitening the noise as

$$\tilde{\boldsymbol{y}}_d^* = \boldsymbol{\Delta}_n^{-1/2}\tilde{\boldsymbol{y}}_d = \boldsymbol{\Delta}_n^{-1/2}\boldsymbol{D}_{\mathrm{eq}}\sqrt{\mathcal{P}_{\mathrm{s}}}\tilde{\boldsymbol{x}}_{\mathrm{s}} + \boldsymbol{\Delta}_n^{-1/2}\mathcal{N}_{\mathrm{eq}}. \tag{15}$$

The symbol detector at the destination estimates each transmitted symbol according to the grouping scheme defined by $\boldsymbol{\Psi}_{\mathrm{m}}$. Every $K$ bits in each group are decoded together with maximum likelihood (ML) criterion

$$\hat{\tilde{\boldsymbol{x}}}_{\mathrm{m}} = \arg\min_{\tilde{\boldsymbol{x}}_i\in\mathcal{A}_K} ||\boldsymbol{\Psi}_{\mathrm{m}}\tilde{\boldsymbol{y}}_d^* - (\boldsymbol{\Psi}_{\mathrm{m}}\boldsymbol{\Delta}_n^{-1/2}\boldsymbol{D}_{\mathrm{eq}})\sqrt{\mathcal{P}_{\mathrm{s}}}\boldsymbol{\Theta}\tilde{\boldsymbol{x}}_i||,$$
$$m \in \{1, \ldots, M\}. \tag{16}$$

Finally, the decoded groups $\hat{\tilde{\boldsymbol{x}}}_{\mathrm{m}}$, $m \in \{0, \ldots, M-1\}$ are reassembled to form the decoded symbol as: $\hat{\tilde{\boldsymbol{x}}} = \sum_{m=1}^{M} \boldsymbol{\Psi}_{\mathrm{m}}^{\mathrm{T}}\hat{\tilde{\boldsymbol{x}}}_{\mathrm{m}}$.

## 4 Performance evaluation

The AsAP system is designed to attain reliable communications by collecting both space and multipath diversity from the sparse UAC channel. In this section, we will analyse the performance of our proposed AsAP protocol. The end-to-end SNR and the average PEP is adopted as the performance metric, and the MCD is derived accordingly.

### 4.1 SNR of AsAP

At the destination of an AsAP system, the equivalent channel response and noise term at the $n$th subcarrier are shown in (13) and (14). The received SNR can be computed as

$$\gamma_{\mathrm{eq}}(n) = \mathbb{E}_{\tilde{\boldsymbol{n}}_{\mathrm{eq}}}\left\{\frac{\mathcal{P}_{\mathrm{s}}(f_n)|\tilde{\boldsymbol{h}}_{\mathrm{eq}}(n)|^2}{|\tilde{\boldsymbol{n}}_{\mathrm{eq}}(n)|^2}\right\}. \tag{17}$$

With the assumption of independent and identically distributed noise with variance $\mathcal{N}(f_n)$ at subcarrier frequency $f_n$, (17) can be expressed as

$$\gamma_{\mathrm{eq}}(n) = \frac{\mathcal{P}_{\mathrm{s}}(f_n)}{\mathcal{N}(f_n)}\frac{\left|\tilde{\boldsymbol{h}}_{sd}(n) + \sum_{r=1}^{R}\boldsymbol{\Omega}_{\mathrm{r}}(n,n)\tilde{\boldsymbol{h}}_{\mathrm{r}d}(n)\boldsymbol{A}_{\mathrm{r}}(n)\tilde{\boldsymbol{h}}_{\mathrm{sr}}(n)\right|^2}{\left|1 + \sum_{r=1}^{R}\boldsymbol{\Omega}_{\mathrm{r}}(n,n)\tilde{\boldsymbol{h}}_{\mathrm{r}d}(n)\boldsymbol{A}_{\mathrm{r}}(n)\right|^2}. \tag{18}$$

Note that the end-to-end SNR depends on the amplification factor, the number of relays and the corresponding relay latency. For a single-relay no-direct-link system with fixed amplification scheme


*IET Commun.*, 2016, Vol. 10, Iss. 6, pp. 677–684

in (6), the end-to-end equivalent SNR can be simplified to

$$\gamma_{\mathrm{eq}}(n)=\frac{\mathcal{P}_{\mathrm{s}}(f_n)}{\mathcal{N}(f_n)}\frac{\left|\tilde{\boldsymbol{h}}_{\mathrm{r}d}(n)\boldsymbol{A}_{\mathrm{r}}(n)\tilde{\boldsymbol{h}}_{\mathrm{sr}}(n)\right|^2}{\left|1+\tilde{\boldsymbol{h}}_{\mathrm{r}d}(n)\boldsymbol{A}_{\mathrm{r}}(n)\right|^2}=\frac{\gamma_{\mathrm{s,r}}(n)\gamma_{\mathrm{r},d}(n)}{\bar{\gamma}_{\mathrm{s,r}}(n)+\gamma_{\mathrm{r},d}(n)+1}, \tag{19}$$

where $\gamma_{i,j}(n)=\mathcal{P}_i(f_n)|\tilde{h}_{i,j}(n)|^2/\mathcal{N}(f_n)$ is the SNR at receiver $j$ due to transmitter $i$ at the $n$th subcarrier, and $\bar{\gamma}_{i,j}(n)$ is the corresponding average SNR. $\mathcal{P}_i(f_n)$ is the transmit power density at node $i$ and subcarrier $n$.

### 4.2 PEP of AsAP

Assume a symbol $\tilde{\boldsymbol{x}}\in\mathcal{A}_K$ is transmitted, and it is erroneously decoded as $\hat{\tilde{\boldsymbol{x}}}$, where $\hat{\tilde{\boldsymbol{x}}}\neq\tilde{\boldsymbol{x}}$ and $\hat{\tilde{\boldsymbol{x}}}\in\mathcal{A}_K$. With ML detection, the corresponding PEP $P_{\mathrm{e}}$ is computed as

$$P_{\mathrm{e}}=P(\tilde{\boldsymbol{x}}\to\hat{\tilde{\boldsymbol{x}}})=Q\left(\sqrt{\frac{d^2(\tilde{\boldsymbol{y}}_d^*,\hat{\tilde{\boldsymbol{y}}}_d^*)}{2\mathcal{N}_0}}\right), \tag{20}$$

where $d(\tilde{\boldsymbol{y}}_d^*,\hat{\tilde{\boldsymbol{y}}}_d^*)=||\tilde{\boldsymbol{y}}_d^*-\hat{\tilde{\boldsymbol{y}}}_d^*||$ is the Euclidean distance between $\tilde{\boldsymbol{y}}_d^*$ and $\hat{\tilde{\boldsymbol{y}}}_d^*$, and $\tilde{\boldsymbol{y}}_d^*=\boldsymbol{\Delta}_n^{-1/2}\boldsymbol{D}_{\mathrm{eq}}\sqrt{\mathcal{P}_{\mathrm{s}}}\tilde{\boldsymbol{x}}$, $\hat{\tilde{\boldsymbol{y}}}_d^*=\boldsymbol{\Delta}_n^{-1/2}\boldsymbol{D}_{\mathrm{eq}}\sqrt{\mathcal{P}_{\mathrm{s}}}\hat{\tilde{\boldsymbol{x}}}$. By defining the error vector $\tilde{\boldsymbol{x}}_{\mathrm{e}}=\tilde{\boldsymbol{x}}-\hat{\tilde{\boldsymbol{x}}}$ and the error matrix $\boldsymbol{D}_{\mathrm{e}}=\mathrm{diag}(\tilde{\boldsymbol{x}}_{\mathrm{e}})$, the Euclidean distance square can be computed as:

$$\begin{aligned}d^2(\tilde{\boldsymbol{y}}_d^*,\hat{\tilde{\boldsymbol{y}}}_d^*)&=||\boldsymbol{\Delta}_n^{-1/2}\boldsymbol{D}_{\mathrm{eq}}\sqrt{\mathcal{P}_{\mathrm{s}}}\tilde{\boldsymbol{x}}_{\mathrm{e}}||^2=||\sqrt{\mathcal{P}_{\mathrm{s}}}\boldsymbol{\Delta}_n^{-1/2}\boldsymbol{D}_{\mathrm{e}}\tilde{\boldsymbol{h}}_{\mathrm{eq}}||^2\\&=\tilde{\boldsymbol{h}}_{\mathrm{eq}}^{\mathrm{H}}\mathcal{P}_{\mathrm{s}}\boldsymbol{\Delta}_n^{-1}|\boldsymbol{D}_{\mathrm{e}}|^2\tilde{\boldsymbol{h}}_{\mathrm{eq}},\end{aligned} \tag{21}$$

where $\tilde{\boldsymbol{h}}_{\mathrm{eq}}$ is the equivalent channel vector in FD

$$\tilde{\boldsymbol{h}}_{\mathrm{eq}}=\tilde{\boldsymbol{h}}_{\mathrm{s}d}+\sum_{r=1}^{R}\boldsymbol{A}_{\mathrm{r}}\boldsymbol{D}_{\mathrm{r}d}\boldsymbol{\Omega}_{\mathrm{r}}\tilde{\boldsymbol{h}}_{\mathrm{sr}}. \tag{22}$$

By using the alternative representation of $Q$ function [31]

$$Q(x)=(1/\pi)\int_0^{\pi/2}\exp\left(-x^2/(2\sin^2\theta)\right)\mathrm{d}\theta, \tag{23}$$

the PEP can be reexpressed as

$$P(\tilde{\boldsymbol{x}}\to\hat{\tilde{\boldsymbol{x}}})=\frac{1}{\pi}\int_0^{\pi/2}\left[\exp\left(-\frac{\tilde{\boldsymbol{h}}_{\mathrm{eq}}^{\mathrm{H}}\mathcal{P}_{\mathrm{s}}\boldsymbol{\Delta}_n^{-1}|\boldsymbol{D}_{\mathrm{e}}|^2\tilde{\boldsymbol{h}}_{\mathrm{eq}}}{4\mathcal{N}_0\sin^2\theta}\right)\right]\mathrm{d}\theta. \tag{24}$$

The average PEP $\bar{P}_{\mathrm{e}}$ for the AsAP system can be computed by averaging over $\tilde{\boldsymbol{h}}_{\mathrm{eq}}$

$$\begin{aligned}\bar{P}_{\mathrm{e}}&=\mathbb{E}_{\tilde{\boldsymbol{h}}_{\mathrm{eq}}}\left[P(\boldsymbol{x}\to\hat{\boldsymbol{x}})\right]\\&=\frac{1}{\pi}\int_0^{\pi/2}\mathbb{E}_{\tilde{\boldsymbol{h}}_{\mathrm{eq}}}\left[\exp\left(-\frac{\tilde{\boldsymbol{h}}_{\mathrm{eq}}^{\mathrm{H}}\mathcal{P}_{\mathrm{s}}\boldsymbol{\Delta}_n^{-1}|\boldsymbol{D}_{\mathrm{e}}|^2\tilde{\boldsymbol{h}}_{\mathrm{eq}}}{4\mathcal{N}_0\sin^2\theta}\right)\right]\mathrm{d}\theta.\end{aligned} \tag{25}$$

To find the average PEP, the statistical property of $\tilde{\boldsymbol{h}}_{\mathrm{eq}}$ needs to be examined. Observe from (22) that conditioned on the R-D channel $\boldsymbol{D}_{\mathrm{r}d}$, $\tilde{\boldsymbol{h}}_{\mathrm{eq}}$ is a complex Gaussian vector with mean $\boldsymbol{\mu}_{\mathrm{eq}}=\boldsymbol{0}$ and covariance matrix $\tilde{\boldsymbol{V}}_{\mathrm{eq}}$. Due to the independency among all channels $\boldsymbol{h}_{i,j}$, $i,j\in\{s,r,d\}$, $\tilde{\boldsymbol{V}}_{\mathrm{eq}}$ can be calculated as:

$$\tilde{\boldsymbol{V}}_{\mathrm{eq}}=\mathbb{E}_{\tilde{\boldsymbol{h}}_{\mathrm{s}d}}\left[\tilde{\boldsymbol{h}}_{\mathrm{s}d}\tilde{\boldsymbol{h}}_{\mathrm{s}d}^{\mathrm{H}}\right]+\sum_{r=1}^{R}\boldsymbol{D}_{\mathrm{r}d}\mathbb{E}_{\tilde{\boldsymbol{h}}_{\mathrm{sr}}}\left[\left(\boldsymbol{A}_{\mathrm{r}}\boldsymbol{\Omega}_{\mathrm{r}}\tilde{\boldsymbol{h}}_{\mathrm{sr}}\right)\left(\boldsymbol{A}_{\mathrm{r}}\boldsymbol{\Omega}_{\mathrm{r}}\tilde{\boldsymbol{h}}_{\mathrm{sr}}\right)^{\mathrm{H}}\right]\boldsymbol{D}_{\mathrm{r}d}^{\mathrm{H}}. \tag{26}$$

Note that the covariance matrix is amplification dependent. We will evaluate the result with the TD-FA scheme for its simplicity. The effects of other amplification schemes will be determined numerically. With TD-FA, (26) can be further simplified as

$$\tilde{\boldsymbol{V}}_{\mathrm{eq}}=\boldsymbol{F}\boldsymbol{V}_{\mathrm{s}d}\boldsymbol{F}^{\mathrm{H}}+\sum_{r=1}^{R}|A_{\mathrm{r}}|^2\left(\boldsymbol{D}_{\mathrm{r}d}\right)\boldsymbol{F}\boldsymbol{V}_{\mathrm{sr}}(\tau_{\mathrm{r}})\boldsymbol{F}^{\mathrm{H}}\left(\boldsymbol{D}_{\mathrm{r}d}\right)^{\mathrm{H}}, \tag{27}$$

where $\boldsymbol{V}_{\mathrm{s}d}$ and $\boldsymbol{V}_{\mathrm{sr}}(\tau_{\mathrm{r}})$ are the diagonal covariance matrices of the S-D channel $\boldsymbol{h}_{\mathrm{s}d}$ and S-R channels $\boldsymbol{h}_{\mathrm{sr}}$ delayed by $\tau_{\mathrm{r}}$, respectively. The ranks of $\boldsymbol{V}_{\mathrm{s}d}$ and $\boldsymbol{V}_{\mathrm{sr}}(\tau_{\mathrm{r}})$ are $L_{\mathrm{s}d,\mathrm{nz}}$ and $L_{\mathrm{sr,nz}}$.

$$\begin{aligned}&\mathbb{E}_{\tilde{\boldsymbol{h}}_{\mathrm{eq}}}\left[\exp\left(-\frac{\tilde{\boldsymbol{h}}_{\mathrm{eq}}^{\mathrm{H}}\mathcal{P}_{\mathrm{s}}\boldsymbol{\Delta}_n^{-1}|\boldsymbol{D}_{\mathrm{e}}|^2\tilde{\boldsymbol{h}}_{\mathrm{eq}}}{4\mathcal{N}_0\sin^2\theta}\right)\right]\\&=\mathbb{E}_{\tilde{\boldsymbol{h}}_{\mathrm{r}d}}\left[\det\left(\boldsymbol{I}+\frac{\mathcal{P}_{\mathrm{s}}}{4\mathcal{N}_0\sin^2\theta}\tilde{\boldsymbol{V}}_{\mathrm{eq}}|\boldsymbol{D}_{\mathrm{e}}|^2\boldsymbol{\Delta}_n^{-1}\right)^{-1}\right].\end{aligned} \tag{28}$$

Then the average PEP can be readily expressed as:

$$\bar{P}_{\mathrm{e}}=\frac{1}{\pi}\int_0^{\pi/2}\mathbb{E}_{\tilde{\boldsymbol{h}}_{\mathrm{r}d}}\left[\det\left(\boldsymbol{I}+\frac{\mathcal{P}_{\mathrm{s}}}{4\mathcal{N}_0\sin^2\theta}\tilde{\boldsymbol{V}}_{\mathrm{eq}}|\boldsymbol{D}_{\mathrm{e}}|^2\boldsymbol{\Delta}_n^{-1}\right)^{-1}\right]\mathrm{d}\theta. \tag{29}$$

In the above equation, $\boldsymbol{D}_{\mathrm{e}}$ and $\boldsymbol{\Delta}_n$ are diagonal matrices. However, due to the correlation among delay taps of the equivalent channel at the destination, the covariance matrix $\tilde{\boldsymbol{V}}_{\mathrm{eq}}$ is not diagonal in general. This renders explicit expression for the average PEP in (29) mathematically intractable. Thus, we will resort to diversity analysis to illustrate the protocol performance.

### 4.3 Diversity of AsAP

In general, the average error performance $\bar{P}_{\mathrm{e}}$ of a communication system can be approximated in terms of $\mathcal{P}/\mathcal{N}_0$ as follows

$$\bar{P}_{\mathrm{e}}\propto\left(G_c\frac{\mathcal{P}}{\mathcal{N}_0}\right)^{-G_d}, \tag{30}$$

where the exponent $G_d$ is referred to as diversity gain and the factor $G_c$ is termed as coding gain. Accordingly, as shown in (29), the diversity gain of an AsAP system is related to the determinant. Though the exact expression of the determinant is not available, we can determine the MCD, which is stated in the following proposition.

*Proposition 1:* (Maximum collectable diversity) The maximum diversity gain of an AsAP system with TD-FA is the minimum of the precoding size and the summation of the number of non-zero taps of the S-D and S-R channels, that is,

$$G_d\leq\min\left\{K,L_{\mathrm{s}d,\mathrm{nz}}+\sum_{r=1}^{R}L_{\mathrm{sr,nz}}\right\} \tag{31}$$

*Proof:* Let $\boldsymbol{T}=\tilde{\boldsymbol{V}}_{\mathrm{eq}}|\boldsymbol{D}_{\mathrm{e}}|^2\boldsymbol{\Delta}_n^{-1}$, then the determinant in (29) can be written as:

$$\det\left(I+\frac{\mathcal{P}_{\mathrm{s}}}{4\mathcal{N}_0\sin^2\theta}T\right)^{-1}=\prod_{i=0}^{K-1}\frac{1}{1+\mathcal{P}_{\mathrm{s}}/\mathcal{N}_0(4\sin^2\theta)\lambda_i}, \tag{32}$$

where $\lambda_i$, $i\in\{0,\ldots,K-1\}$ are non-increasing eigenvalues of matrix $\boldsymbol{T}$. Suppose the rank of $\boldsymbol{T}$ is $r$, then there are $r$ non-zero $\lambda_i$, thus (32)

can be rewritten as:

$$\det\left(\boldsymbol{I}+\frac{\mathcal{P}_{\mathrm{s}}}{4\mathcal{N}_0\sin^2\theta}\boldsymbol{T}\right)^{-1}=\prod_{i=0}^{r-1}\left(1+\frac{\mathcal{P}_{\mathrm{s}}}{\mathcal{N}_0(4\sin^2\theta)}\lambda_i\right)^{-1}\leq\left(\prod_{i=0}^{r-1}\frac{\lambda_i}{4\sin^2\theta}\right)\left(\frac{\mathcal{P}_{\mathrm{s}}}{\mathcal{N}_0}\right)^{-r}. \quad (33)$$

Recall the definition in (30), the diversity gain of the AsAP system is $r$. In matrix $\boldsymbol{T}$, $\boldsymbol{\Delta}_n^{-1}$ is diagonal with full rank of $K$. In addition, according to the precoding matrix design [24], $\boldsymbol{D}_{\mathrm{e}}=\mathrm{diag}(\Theta\boldsymbol{x}_{\mathrm{e}})$ is also of full rank for any error pairs. Thus the rank of $\boldsymbol{T}$ is determined by the rank of $\tilde{\boldsymbol{V}}_{\mathrm{eq}}$, that is, $\mathrm{rank}(\boldsymbol{T})=\mathrm{rank}(\tilde{\boldsymbol{V}}_{\mathrm{eq}}|\boldsymbol{D}_{\mathrm{e}}|^2\boldsymbol{\Delta}_n^{-1})=\mathrm{rank}(\tilde{\boldsymbol{V}}_{\mathrm{eq}})$. For TD-FA, $\tilde{\boldsymbol{V}}_{\mathrm{eq}}$ is shown in (27). Note that both $\boldsymbol{F}$ and $\boldsymbol{D}_{rd}$ are of full rank, and the rank of $\boldsymbol{V}_{sd}$ and $\boldsymbol{V}_{\mathrm{sr}}$ are $L_{sd,\mathrm{nz}}$ and $L_{\mathrm{sr,nz}}$, respectively. According to the rank property of matrix summation, we can obtain that $\mathrm{rank}(\tilde{\boldsymbol{V}}_{\mathrm{eq}})\leq L_{sd,\mathrm{nz}}+\sum_{r=1}^{R}L_{\mathrm{sr,nz}}$. In addition, the size of $\tilde{\boldsymbol{V}}_{\mathrm{eq}}$ is $K\times K$, thus the MCD is also limited by the precoding size $K$. Therefore, the MCD of the AsAP system is the minimum of $K$ and $\mathrm{rank}(\tilde{\boldsymbol{V}}_{\mathrm{eq}})$.

Several remarks for this proposition are listed in order here.

*4.3.1 MCD achievability:* To collect the maximum multipath diversity, the rank of the covariance matrix $\tilde{\boldsymbol{V}}_{\mathrm{eq}}$ in (27) needs to equal the sum $L_{sd,\mathrm{nz}}+\sum_{r=1}^{R}L_{\mathrm{sr,nz}}$, and the precoding size $K$ should be no less than this sum. Note that Proposition 1 is valid for any R-D channel statistics. In a special case where the R-D channel $\tilde{\boldsymbol{h}}_{rd}$ is deterministic and non-frequency-selective, namely $\boldsymbol{D}_{rd}=D_{rd}\boldsymbol{I}$, we have

$$\tilde{\boldsymbol{V}}_{\mathrm{eq}}=\mathbf{F}\left[\boldsymbol{V}_{sd}+\sum_{r=1}^{R}|A_{\mathrm{r}}D_{rd}|^2\boldsymbol{V}_{\mathrm{sr}}(\tau_{\mathrm{r}})\right]\boldsymbol{F}^{\mathrm{H}}. \quad (34)$$

If the S-D channel $\tilde{\boldsymbol{h}}_{sd}$ and the S-R channels $\tilde{\boldsymbol{h}}_{\mathrm{sr}}$ with delay $\tau_{\mathrm{r}}$ are perfectly separated with no overlap, then the rank of $\tilde{\boldsymbol{V}}_{\mathrm{eq}}$ is the sum of all non-zero taps of S-D and S-R links. Thus the maximum diversity can be collected. For Rayleigh-fading R-D channels, the achievability of MCD is not analytically explicit. It will be revealed by simulations in the next section. In addition, the precoding size needs to be sufficiently large to collect the full diversity provided by the channel. However, larger $K$ requires more computation energy. Henceforth, in practical systems, there is a trade-off between diversity collection and energy consumption.

*4.3.2 Underwater acoustic channel:* In UAC, channel taps are sparse in nature [29]. Thus in an AsAP system, the relay channels associated with random delays are very likely to be separated. This allows the system to collect space diversity in the form of multipath diversity. Therefore, our AsAP protocol is inherently suitable for UAC. Furthermore, in a single-relay system without direct link, as the number of non-zero S-R channel taps increases, the MCD increases linearly. However, in a multi-relay system, as the number of relays increases, the chance of channel tap collision increases. The collectable diversity will not increase linearly as the number of relays.

*4.3.3 Effect of the amplification factor:* The result in Proposition 1 is derived based on the fixed amplification scheme (TD-FA). For other amplification schemes, the MCD is not explicit from the average PEP formula. However, note that the amplification factor will not change the number of independent channel taps, thus the MCD of other amplification schemes will not exceed the value derived for TD-FA in (31). We will verify the effects of different amplification schemes in the next section.

## 5 Simulations

In this section, we simulate the performance of RA-UAC systems with the AsAP protocol. Through comparisons among different scenarios, the benefits of the AsAP design are verified. In addition, the effects of the number of relays and channel taps, and amplification factors will also be discussed.

### 5.1 Simulation setup

Consider an AsAP system with S-D distance of $D=1000$ m and mid-point relay. In all simulations, binary phase shift keying signalling is used and bit error rate (BER) is recorded to demonstrate the performance. The OFDM precoding size is chosen to be $K=8$. The OFDM symbol size is $N=1024$. We use the UAC channel model described in Section 2.2, with the reflection loss being $\Gamma_l=1/\sqrt{2}$ for all paths as in [4].

### 5.2 Results and comparisons

*5.2.1 Benefits of relaying and precoding:* Compared with traditional direct-link communications, our AsAP protocol adopts relays to assist data communications and chooses OFDM precoding to collect multipath diversity. Thus we first verify the benefits of these two techniques. For a water depth of 30 m, which generates all channels with two non-zero taps, we simulate the BER performance of the direct-link system and our AsAP system with and without precoding. The results are shown in Fig. 3. By comparing both systems without precoding, we note that the AsAP system achieves much better performance with about 8 dB coding gain, though both of them have the same diversity gain of 1. By adding the precoding, the direct-link system achieves a diversity gain of 2, which equals to the number of channel taps. For the AsAP system, the precoding collects a diversity gain of 3, which is less than the MCD of 4. The comparison shows that the AsAP system excels the direct-link system with both higher diversity gain and larger coding gain.

*5.2.2 Effect of number of channel taps:* The remarks of Proposition 1 indicate that, for a single-relay AsAP system without direct link, the MCD increases linearly with the number of taps of the S-R channel. Since the number of channel taps changes with water depth, we simulate an AsAP system with one relay at different water depths to verify its diversity collection. The BER curves are plotted in Fig. 4. As water depth decreases from 50–5 m, the number of non-zero channel taps increase from 1–5. Observe from the figure that the AsAP system indeed collects a diversity order the same as the corresponding number of non-zero taps of the

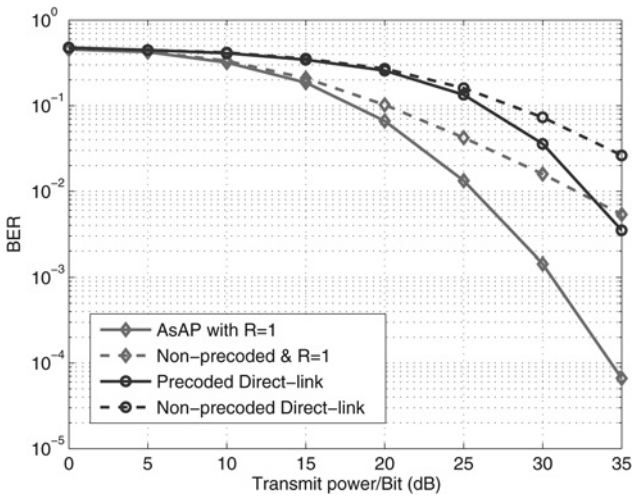


**Fig. 3** *BER performance for direct-link systems and AsAP systems with and without precoding. The water depth is 30 m*


*IET Commun.*, 2016, Vol. 10, Iss. 6, pp. 677–684

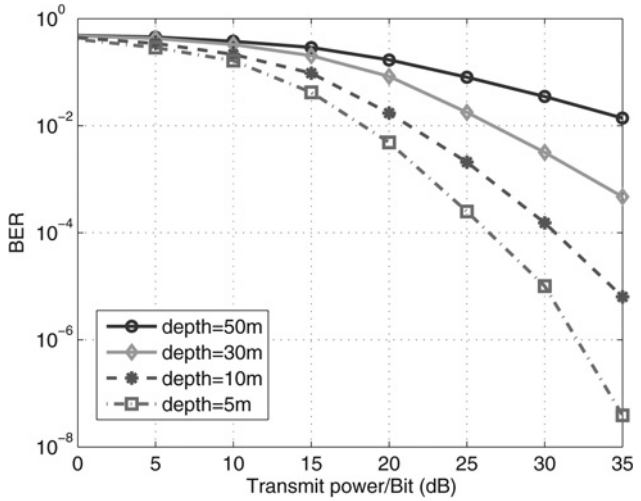


**Fig. 4** *BER performance for AsAP systems with different number of channel taps. Assume there is no direct link and R = 1*

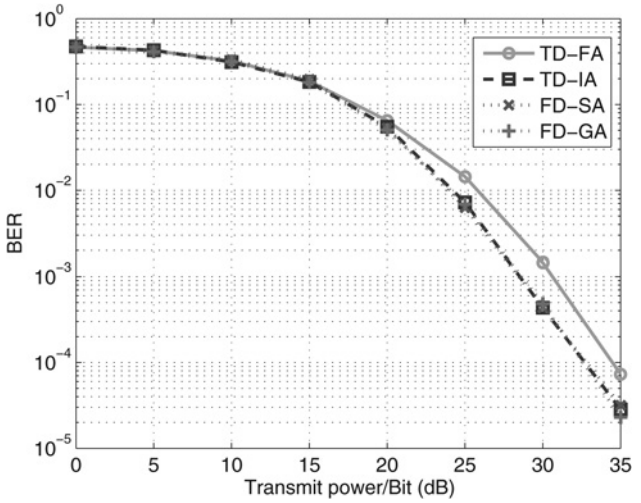


**Fig. 6** *BER performance for AsAP systems with different amplification schemes. The water depth is 30 m and R = 1*

S-R channel. This observation also proves that the MCD is achievable under Rayleigh fading R-D channels.

*5.2.3 Effect of number of relays R:* Recall that, in multi-relay AsAP systems, the MCD will not increase linearly with the number of relays if channel tap collision exists. In Fig. 5, we plot the BER curves for AsAP systems with different relays at a water depth of 30 m. The results show that the diversity gains for the AsAP systems with $R = 1$, 2 and 3 are 2, 3 and 4, respectively. This indicates that the diversity gain increases with the number of relay, yet not linearly.

*5.2.4 Effect of amplification factor:* In all simulations above, the adopted amplification scheme is TD-FA. In Fig. 6, we plot the performance of AsAP systems with all four amplification schemes: TD-FA, TD-IA, FD-SA and FD-GA at a water depth of 30 m. This figure reveals that all schemes collect similar diversity order, which confirms our remark of Proposition 1 that the diversity order of other amplification schemes will not exceed the MCD of the system with TD-FA. The only difference of these schemes is coding gain. Interestingly, all three instantaneous schemes have exactly the same performance and they exhibit about 2 dB coding gain over TD-FA. This confirms that the instantaneous amplification schemes achieve better performance over the fixed TD-FA scheme. However, the higher computation cost and larger signal processing delay induced by the instantaneous schemes render a trade-off between system performance and complexity.

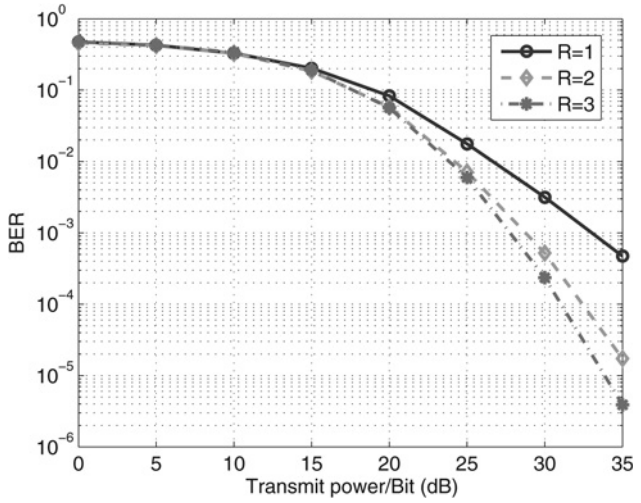


**Fig. 5** *BER performance for AsAP systems with different number of relays and with no direct link. The water depth is 30 m*

## 6 Conclusions

In this paper, we designed a practical asynchronous RA-UAC protocol (AsAP) tailored for underwater systems. The new protocol resolves both the time synchronisation difficulty and frequency-selectivity issue of UAC channels. In the meantime, it exploits the sparsity feature of underwater channels. To improve communication efficiency, full-duplex relay scheme can be adopted. The performance of the AsAP protocol was evaluated with end-to-end SNR, the average PEP and the maximum collectable diversity. Simulations were conducted to verify the merits of the AsAP protocol and to reveal the effects of system parameters. Results indicate that both diversity gain and coding gain are achieved from OFDM precoding and relaying; the collectable diversity increases linearly with the number of channel taps but not linearly with the number of relays; the amplification factor affects only the coding gain but not diversity gain.

## 7 Acknowledgment

We would like to take the opportunity to thank Mr Pan Deng for his help in our simulations.

## 8 References

1 Akyildiz, I., Pompili, D., Melodia, T.: 'Underwater acoustic sensor networks: Research challenges', *Elsevier's J. Ad Hoc Netw.*, 2005, **3**, pp. 257–279
2 Heidemann, J., Ye, W., Wills, J., *et al.*: 'Research challenges and applications for underwater sensor networking'. Proc. of Wireless Communications and Networking Conf., 1, Las Vegas, Nevada, 3–6 April 2006, pp. 228–235
3 Syed, A., Heidemann, J.: 'Time synchronization for high latency acoustic networks'. Proc. of Int. Conf. on Computer Communications, Barcelona, Spain, 23–29 April 2006, pp. 1–12
4 Vajapeyam, M., Vedantam, S., Mitra, U., *et al.*: 'Distributed space-time cooperative schemes for underwater acoustic communications', *IEEE J. Ocean. Eng.*, 2008, **33**, (4), pp. 489–501
5 Aval, Y.M., Stojanovic, M.: 'Differentially coherent multichannel detection of acoustic OFDM signals', *IEEE J. Ocean. Eng.*, 2015, **40**, (2), pp. 251–268
6 Salim, A., Duman, T.M.: 'An asynchronous two-way relay system with full delay diversity in time-varying multipath environments'. Int. Conf. on Computing, Networking and Communications (ICNC), Garden Grove, California, 16–19 February 2015, pp. 900–904
7 Qu, F., Yang, L.: 'Basis expansion model for underwater acoustic channels?' Proc. of MTS/IEEE Oceans Conf., Quebec, Canada, 15–18 September 2008, pp. 1–7

8 Cho, W., Cao, R., Yang, L.: 'Optimum resource allocation for amplify-and-forward relay networks with differential modulation', *IEEE Trans. Signal Process.*, 2008, **56**, (11), pp. 5680–5691
9 Laneman, J.N., Tse, D.N.C., Wornell, G.W.: 'Cooperative diversity in wireless networks: Efficient protocols and outage behavior', *IEEE Trans. Inf. Theory*, 2004, **50**, (12), pp. 3062–3080
10 Babu, A., Joshy, S.: 'Maximizing the data transmission rate of a cooperative relay system in an underwater acoustic channel', *Int. J. Commun. Syst.*, 2012, **25**, pp. 231–253
11 Chao, G., Liu, Z., Cao, B., *et al*.: 'Relay selection scheme based on propagation delay for cooperative underwater acoustic network'. 2013 Int. Conf. on Wireless Communications and Signal Processing (WCSP), Hangzhou, China, 24–26 October 2013, **39**, pp. 331–342
12 Kam, C., Kompella, S., Nguyen, G., *et al*.: 'Frequency selection and relay placement for energy efficiency in underwater acoustic networks', *IEEE J. Ocean. Eng.*, 2013, pp. 1–12
13 Karakaya, B., Hasna, M., Uysal, M., *et al*.: 'Relay selection for cooperative underwater acoustic communication systems'. 2012 19th Int. Conf. on Telecommunications (ICT), Jounieh, Lebanon, 23–25 April 2012, pp. 1–6
14 Wang, P., Zhang, X.: 'Energy-efficient relay selection for qos provisioning in mimo-based underwater acoustic cooperative wireless sensor networks'. Proc. of Conf. on Info. Sciences and Systems, Baltimore, MD, 20–22 March 2013
15 Wei, Y., Kim, D.: 'Exploiting cooperative relay for reliable communications in underwater acoustic sensor networks'. IEEE Military Communications Conf. (MILCOM), Baltimore, MD, 6–8 October 2014, pp. 518–524
16 Wang, P., Zhang, X., Song, M.: 'Doppler compensation based optimal resource allocation for qos guarantees in underwater mimo-ofdm acoustic wireless relay networks'. Proc. of Military Communication Conf., San Diego, CA, 18–20 November 2013
17 Murphy, C., Walls, J., Schneider, T., *et al*.: 'Capture: A communications architecture for progressive transmission via underwater relays with eavesdropping', *IEEE J. Ocean. Eng.*, 2013, **39**, pp. 120–130
18 Wei, S., Goeckel, D.L., Valenti, M.C.: 'Asynchronous cooperative diversity', *IEEE Trans. Wirel. Commun.*, 2006, **5**, pp. 1547–1557
19 Razak, N.A., Said, F., Aghvami, A.H.: 'Performance of relay cyclic delay diversity in multicarrier system'. IEEE 20th Int. Symp. on Personal, Indoor and Mobile Radio Communications, 1, Tokyo, Japan, 13–16 September 2009, pp. 2025–2029
20 Slimane, S.B., Osseiran, A.: 'Relay communciation with delay diversity for future communication systems'. Proc. of Vehicular Technology Conf., Montreal, Canada, 25–28 September 2006, pp. 1–5
21 Han, Z., Sun, Y.L., Shi, H.: 'Cooperative transmission for underwater acoustic communications'. Proc. of Int. Conf. on Communications, Beijing, China, 19–23 May 2008, pp. 2028–2032
22 Wang, P., Feng, W., Zhang, L., *et al*.: 'Asynchronous cooperative transmission in underwater acoustic networks'. IEEE Symp. on Underwater Technology (UT) and Workshop on Scientific Use of Submarine Cables and Related Technologies (SSC), Tokyo, Japan, 5–8 April 2011
23 Carbonelli, C., Mitra, U.: 'A simple sparse channel estimator for underwater acoustic channels'. Proc. of Oceans Conf., Vancouver, Canada, 29 September–4 October 2007, pp. 1–68
24 Liu, Z., Xin, Y., Giannakis, G.B.: 'Linear constellation precoding for OFDM with maximum multipath diversity and coding gains', *IEEE Trans. Commun.*, 2003, **51**, (3), pp. 416–427
25 Riihonen, T., Werner, S., Wichman, R.: 'Mitigation of loopback self-interference in full-duplex MIMO relays', *IEEE Trans. Signal Process.*, 2011, **59**, (12), pp. 5983–5993
26 Cui, H., Song, L., Jiao, B.: 'Relay selection for two-way full duplex relay networks with amplify-and-forward protocol', *IEEE Trans. Wirel. Commun.*, 2014, **13**, (7), pp. 3768–3876
27 Berkhovskikh, L., Lysanov, Y.: 'Fundamentals of ocean acoustics' (Springer, New York, 1982)
28 Stojanovic, M.: 'On the relationship between capacity and distance in an underwater acoustic communication channel'. Proc. of Int. Workshop on Underwater Networks, Los Angeles, California, 25 September 2006, pp. 41–47
29 Berger, C.R., Zhou, S., Preisig, J.C., *et al*.: 'Sparse channel estimation for multicarrier underwater acoustic communication: From subspace methods to compressed sensing', *IEEE Trans. Signal Process.*, 2010, **58**, pp. 1708–1721
30 Zielinski, A., Yoon, Y.-H., Wu, L.: 'Performance analysis of digital acoustic communication in a shallow water channel', *IEEE J. Ocean. Eng.*, 1995, **20**, pp. 293–299
31 Craig, J.W.: 'A new, simple and exact result for calculating the probability of error for two-dimensional signal constellations'. Proc. of Military Communication Conf., 2, McLean, VA, 4–7 November 1991, pp. 571–575